EUROPEAN ORGANIZATION FOR NUCLEAR RESEARCH

CERN-EP/89-25
January 31st, 1989

Measurements of the u Valence Quark Distribution Function in the Proton and u Quark Fragmentation Functions

The European Muon Collaboration

Aachen[1], CERN[2], DESY (Hamburg)[3], Freiburg[4], Hamburg (University)[5], Kiel[6], LAL (Orsay)[7], Lancaster[8], LAPP (Annecy)[9], Liverpool[10], Marseille[11], Mons[12], MPI (München)[13], Oxford[14], RAL (Chilton)[15], Sheffield[16], Torino[17], Uppsala[18], Warsaw[19], Wuppertal[20]

M. Arneodo[17], A. Arvidson[18], J.J. Aubert[11], B. Badelek[19a)], J. Beaufays[2], C.P. Bee[10], C. Benchouk[11], G. Berghoff[1], I.G. Bird[8b)], D. Blum[7], E. Böhm[6], X. de Bouard[9+], F.W. Brasse[3], H. Braun[20], C. Broll[9+], S.C. Brown[10c)], H. Brück[20d)], H. Calen[18], J.S. Chima[15e)], J. Ciborowski[19a)], R.Clifft[15], G. Coignet[9], F. Combley[16], J. Coughlan[8f)], G.d'Agostini[11], S. Dahlgren[18], F. Dengler[13], I. Derado[13] T. Dreyer[4], J. Drees[20], M. Düren[1], V. Eckardt[13], A. Edwards[20g)], M. Edwards[15], T. Ernst[4], G. Eszes[9h], J. Favier[9], M.I. Ferrero[17], J. Figiel[5i)], W. Flauger[3], J. Foster[16j)] E. Gabathuler[10], J. Gajewski[5a)], R. Gamet[10], J. Gayler[3], N. Geddes[14f)], P. Grafström[18o)], F. Grard[12], J. Haas[4], E. Hagberg[18], F.J. Hasert[1k)], P. Hayman[10], P. Heusse[7], M. Jaffre[7], A. Jacholkowska[2l)], F. Janata[5m)], G. Jancso[13h)], A.S. Johnson[14n)], E.M. Kabuss[4b)], G. Kellner[2], V. Korbel[3], A. Krüger[17], J. Krüger[3], S. Kullander[18], U. Landgraf[4], D. Lanske[1], J. Loken[14], K. Long[14o)], M. Maire[9], P. Malecki[13], A. Manz[13], S. Maselli[13], W. Mohr[4], F. Montanet[11o)], H.E. Montgomery[2p)], E. Nagy[9h)], J. Nassalski[19q)], P.R. Norton[15], F.G. Oakham[15r)], A.M. Osborne[2], C. Pascaud[7], B. Pawlik[13], P. Payre[11], C. Peroni[17], H. Peschel[20], H. Pessard[9], J. Pettingale[10], B. Pietrzyk[11], B. Poensgen[5], M. Pötsch[20], P. Renton[14], P. Ribarics[9h)], K. Rith[4b)], E. Rondio[19a)], A. Sandacz[19q)], M. Scheer[1], A. Schlagböhmer[4], H. Schiemann[5], N. Schmitz[13], M. Schneegans[9], M. Scholz[1], M. Schouten[13], T. Schröder[4], K. Schultze[1], T. Sloan[8], H.E. Stier[4], M. Studt[5], G.N. Taylor[14s)], J.M. Thenard[9], J.C. Thompson[15], A. de la Torre[5t)], J. Toth[9h)], L. Urban[1], L. Urban[9h)], W. Wallucks[4], M. Whalley[16u)], S. Wheeler[16], W.S.C. Williams[14], S.J. Wimpenny[10n)], R. Windmolders[12], G. Wolf[13].

(Submitted to Nuclear Physics B)

ABSTRACT

A new determination of the u valence quark distribution function in the proton is obtained from the analysis of identified charged pions, kaons, protons and antiprotons produced in muon-proton and muon-deuteron scattering. The comparison with results obtained in inclusive deep inelastic lepton-nucleon scattering provides a further test of the quark-parton model. The u quark fragmentation functions into positive and negative pions, kaons, protons and antiprotons are also measured.

For footnotes see next page

Addresses

1) III Physikalisches Institut A, Physikzentrum, RWTH, D-5100 Aachen, FRG.
2) CERN, CH-1211 Geneva 23, Switzerland.
3) DESY, D-2000 Hamburg, FRG.
4) Fakultät für Physik, Universität Freiburg, D-7800 Freiburg, FRG.
5) II Institut für Experimentalphysik, Universität Hamburg, D-2000, FRG.
6) Institut für Kernphysik, Universität Kiel, D-2300 Kiel, FRG.
7) Laboratoire de l'Accélérateur Linéaire, Université de Paris-Sud, F-914005 Orsay, France.
8) Department of Physics, University of Lancaster, Lancaster LA1 4YB, UK.
9) Laboratoire d'Annecy-le-Vieux de Physique des Particules, B.P. 909, F-74019, Annecy-le-Vieux, Cedex, France.
10) Department of Physics, University of Liverpool, Liverpool L69 3BX, UK.
11) Centre de Physique des Particules, Faculté des Sciences de Luminy, F-13288
12) Faculté des Sciences, Université de l'Etat à Mons, B-7000 Mons, Belgium.
13) Max-Planck-Institut für Physik and Astrophysik, D-8000 München, FRG.
14) Nuclear Physics Laboratory, University of Oxford, Oxford OX1 3RH, UK.
15) Rutherford and Appleton Laboratory, Chilton, Didcot OX1 0QX, UK.
16) Department of Physics, University of Sheffield, Sheffield S3 7RH, UK.
17) Istituto di Fisica, Università di Torino, I-10125, Italy.
18) Department of Radiation Science, University of Uppsala, S-75121 Uppsala, Sweden.
19) Physics Institute, University of Warsaw and Institute for Nuclear Studies, 00681 Warsaw, Poland.
20) Fachbereich Physik, Universität Wuppertal, D-5600 Wuppertal, FRG.

a) University of Warsaw, Poland.
b) Now at MPI für Kernphysik, Heidelberg, FRG.
c) Now at TESA S.A., Renens, Switzerland.
d) Now at DESY, Hamburg, FRG.
e) Now at British Telecom, London, UK.
f) Now at RAL, Chilton, Didcot, UK.
g) Now at Jet, Joint Undertaking, Abingdon, UK.
h) Permanent address: Central Research Institute for Physics, Hungarian Academy of Science, Budapest, Hungary.
i) Now at Institute of Nuclear Physics, Krakow, Poland.
j) Now at University of Manchester, UK.
k) Now at Krup Atlas Elektronik GmbH, Bremen, FRG.
l) Now at Laboratoire de l'Accélérateur Linéaire, Université de Paris-Sud, Orsay, France.
m) Now at Beiersdorf AG, Hamburg, FRG.
n) Now at SLAC, Stanford, California, USA.
o) Now at CERN, Genève, Switzerland.
p) Now at FNAL, Batavia, Illinois, USA.
q) Institute for Nuclear Studies, Warsaw, Poland.
r) Now at NRC, Ottawa, Canada.
s) Now at University of Melbourne, Parkville, Victoria, Australia.
t) Now at Universidad Nacional, Mar del Plata, Argentina.
u) Now at University of Durham, UK.
+) Deceased.

1. INTRODUCTION

Experiments on deep inelastic lepton-nucleon scattering are well suited to investigate both nucleon structure as well as the process of hadronization. These experiments have revealed the partonic composition of the nucleon and allowed the study of how the parton systems (quarks, diquarks and gluons) evolve towards observable hadrons. At presently available energies hadron production in deep inelastic scattering can be viewed in the framework of the quark-parton model (QPM) as a two stage process. In the first stage, on a scale down to distances of 10^{-2} fm, the lepton-quark scattering, mediated by the exchange of a virtual boson, takes place. Subsequently in the second stage, on the distance scale of > 1 fm, the partonic systems evolve into final state hadrons. The measured hadron distributions are expected to reflect both stages.

In this paper we present results on both these stages obtained in the analysis of final state hadrons in 280 GeV muon-proton and muon-deuteron interactions. The experiment was designed to study hadron final states with almost complete acceptance and a set of detectors allowing particle identification over a large kinematic range. The first result presented here is the scaled-momentum distribution of the u valence quarks in the proton. This distribution was extracted from the differences of the distributions obtained for positive and negative pions, kaons and protons in the hydrogen and deuterium data. The second result is a measurement of the u quark fragmentation functions into charged pions, kaons, protons and antiprotons extracted from the data and obtained in a kinematic region where the QCD corrections are small.

The valence quark distributions $xu_v(x)$ and $xd_v(x)$ have been previously measured in experiments on inclusive deep inelastic neutrino and muon scattering [1-4]. Neutrino and antineutrino measurements on hydrogen were made by the CDHS collaboration and by the CERN experiment WA21, and on deuterium by the experiment WA25. The EMC NA2 experiment obtained quark distributions from data on muon scattering in hydrogen and deuterium.

The measurement of $xu_v(x)$ presented in this paper was obtained by a different method from that used in the previous experiments. In principle, it is also possible to extract the $xd_v(x)$ distribution using the same method, but with errors much larger than those for $xu_v(x)$. Due to the limited statistics of the present data, the comparison with other results on $xd_v(x)$ is not meaningful.

Most data on quark fragmentation functions come from experiments on e^+e^- annihilation at PETRA and PEP [5]. However, except for the particular case of the c quark fragmentation [6], such experiments only allow the fragmentation functions to be determined in a model dependent way. The e^+e^- annihilation at the energies of PETRA and PEP (29-35 GeV) proceeds through the creation of quark-antiquark pairs of different flavours. Thus the observed hadron distributions are averages of fragmentation functions of the different flavours.

Deep inelastic scattering experiments with neutrinos have the advantage of selecting the flavour of the fragmenting quarks using different types of beams and targets (neutrino or antineutrino, hydrogen or deuterium). Results have been published [7] on the comparison of the u and d quark fragmentation functions into charged pions. However, in that experiment the pion distributions were extracted from the distributions of unidentified hadrons using a model dependent correction for the kaon and proton contributions.

In our previous muon experiment (NA2) particle identification was limited essentially to forward emitted protons. Details of quark fragmentation into protons and antiprotons were studied [8] and the u quark fragmentation functions into charged pions were measured [9].

The present experiment, in addition to a better determination of the hadron variables, combines the advantages of controlling the flavour of the scattered quark (by the scaling variable x) with hadron identification. Some results on the production of identified hadrons in this experiment have already been published [10-12].

In the following section we describe briefly the experimental details. Section 3 describes the method used to extract the valence quark distributions, the $xu_V(x)$ distribution is presented and compared to other experiments. In section 4 the quark fragmentation functions into positive and negative pions and kaons as well as into protons and antiprotons are presented.

2. EXPERIMENTAL PROCEDURE

The data used in this analysis were obtained in a deep inelastic muon-nucleon scattering experiment performed at the CERN SPS (experiment NA9). A 280 GeV beam of positive muons is incident on a one metre long target of liquid hydrogen or deuterium which is surrounded by a streamer chamber, which in turn is positioned inside a superconducting vertex spectrometer magnet (VSM). The scattered muon and hadrons with momenta greater than about 5 GeV pass through a second magnet, the forward spectrometer magnet (FSM). The two magnets are instrumented with proportional and drift chambers. The apparatus is triggered by fast scintillator hodoscopes when a muon is scattered through more than 1/2°. A detailed description of the detector [13] and subsequent analysis [10] (see also references quoted therein) can be found in previous publications.

In order to restrict the data to kinematic regions where radiative and acceptance corrections are small, the following cuts on the event variables were used:

$$Q^2 > 4\ \mathrm{GeV}^2$$
$$20 < \nu < 260\ \mathrm{GeV}$$
$$16 < W^2 < 400\ \mathrm{GeV}^2$$
$$\nu < 0.9\ E_\mu$$
$$E'_\mu > 20\ \mathrm{GeV}$$
$$\theta_\mu > 0.75°$$
$$x > 0.01$$

where $-Q^2$ and ν are the four-momentum squared and the laboratory energy transferred between the incident and scattered muons, W is the total centre of mass energy of the secondary hadrons, E_μ and E_μ' are the incident and scattered muon energies, θ_μ is the muon scattering angle and x is the Bjorken scaling variable. The number of events surviving these cuts is 25546 for the hydrogen target and 20631 for the deuterium target.

The longitudinal distributions of the final state hadrons are expressed in terms of $x_F = 2\ p_L/W$ (x-Feynman) and $z = E_h/\nu$, where p_L is the hadron momentum component parallel to the virtual photon direction in the centre of mass system of the virtual photon and the target nucleon, and E_h is the hadron energy in the laboratory system.

Charged particle identification is provided by an extensive set of detectors. A time-of-flight hodoscope system, two silica aerogel Cerenkov counters and two gas Cerenkov counters cover the low and intermediate momentum range. A large gas Cerenkov counter is used to identify fast hadrons in the forward spectrometer. This set of detectors allows identification of pions, kaons and protons in a substantial part of the momentum range between 600 MeV and 80 GeV.

For each track the probability of obtaining the observed signal (pulse height or time-of-flight) for an assumed particle mass (e, π, K, p) is determined for each counter taking into account counter efficiencies and background contributions. For tracks passing through more than one counter the probabilities are multiplied. The selection of different particles is defined by cuts on these probabilities. The cuts were determined by a Monte Carlo simulation and were adjusted in order to optimise the identification efficiency and minimise the background [10]. After the cuts the contamination of misidentified particles is less than 10% in the final samples of pions and protons and is less than 20% in the sample of kaons. This system allows identification of roughly 50% of all charged hadrons. Table 1 contains the numbers of identified particles obtained from each target.

A detailed Monte Carlo simulation of the experiment was used to correct the data for radiative effects, trigger acceptance, acceptance losses, particle misidentification and reconstruction efficiencies. Monte Carlo events were generated according to the Lund model [14], followed by a full simulation of detector responses and then processed in the same way as the real events. A global acceptance A(y) for a distribution of hadrons of a given species and charge in a given variable y was calculated as the ratio of the distribution obtained after the apparatus simulation to the distribution for the generated events. A measured hadron distribution is corrected according to the formula

$$f_c(y) = f_m(y) \,/\, A(y)$$

where f_c denotes the corrected distribution and f_m the measured distribution.

For the analysis described in this paper the acceptance as a function of x_F for different hadron species is shown in fig. 1. It is dominated by the limited momentum ranges for particle identification and the geometrical acceptance of the time-of-flight and Cerenkov counters. In general the acceptance is higher for the hadrons emitted in the forward hemisphere ($x_F > 0$). Only these hadrons will be used in the analysis described in the following sections.

3. EXTRACTION OF THE U VALENCE QUARK DISTRIBUTION FUNCTION

In the quark-parton model (QPM) the normalised cross section for charged lepto-production of a given hadron h, emitted in the forward hemisphere in the virtual photon-nucleon centre of mass system, is given by

$$\frac{1}{\sigma_{DIS}(x)} \frac{d\sigma^{h}(x,z)}{dz} = \frac{1}{N_{\mu}(x)} \frac{dN^{h}(x,z)}{dz} = \frac{\sum_f e_f^2 q_f(x) D_f^h(z)}{\sum_f e_f^2 q_f(x)} = \frac{x \sum_f e_f^2 q_f(x) D_f^h(z)}{F_2(x)} \qquad (1)$$

In this formula N_{μ} and N^h are respectively the number of deep inelastic events and the number of produced hadrons, e_f and $q_f(x)$ are the charge and the scaled-momentum distribution function of (anti)quarks of flavour f in the proton, $D_f^h(z)$ is the fragmentation function of the (anti)quark f into hadrons of type h and $F_2(x)$ is the nucleon structure function.

Assuming charge conjugation symmetry for the fragmentation functions and the equality of sea quark and antiquark distribution functions for each flavour, the contribution of the sea quarks of a given flavour to the production of a given hadron is the same as the contribution of the corresponding antiquarks to the production of a hadron of opposite sign. Thus, only the valence quarks contribute to the differences of the distributions of hadrons of opposite charges.

This leads to the following expressions for the differences of the distributions of hadrons of opposite charges produced on the proton [15]

$$N_H^{\pi^+}(x,z) - N_H^{\pi^-}(x,z) = \frac{\frac{1}{9}[4xu_v(x) - xd_v(x)]}{F_2^H(x)} [D_u^{\pi^+}(z) - D_u^{\pi^-}(z)] \qquad (2a)$$

$$N_H^{p}(x,z) - N_H^{\bar{p}}(x,z) = \frac{\frac{1}{9}[4xu_v(x) + xd_v(x)]}{F_2^H(x)} [D_u^{p}(z) - D_u^{\bar{p}}(z)] \qquad (2b)$$

$$N_H^{K^+}(x,z) - N_H^{K^-}(x,z) = \frac{\frac{1}{9}4xu_v(x)}{F_2^H(x)} \; [D_u^{K^+}(z) - D_u^{K^-}(z)] \qquad (2c)$$

where $N^h(x,z) = (1/N_\mu(x))\,(dN^h(x,z)/dz)$, u_v and d_v are the valence quark distributions and the index H indicates the hydrogen target. The above formulae were obtained assuming charge conjugation invariance and isospin rotation symmetry for the quark fragmentation functions (e.g. $D_u^{\pi^+} = D_d^{\pi^-}$, $D_u^{\pi^-} = D_d^{\pi^+}$) as well as the hypothesis that the so-called unfavoured fragmentation functions for the production of hadrons of a given type are equal (e.g. $D_u^{K^-} = D_d^{K^+} = D_d^{K^-}$). For equation (2b) we have made the additional assumptions that $D_u^{\bar{p}} = D_d^{\bar{p}}$ and $D_u^p = D_d^p$. We will discuss later a possible systematic error due to the latter assumption.

The differences $N^{h^+} - N^{h^-}$, where h = π, K, p, are seen to factorise into two terms, one depending on the Bjorken x variable and the other on the fraction of the scattered quark energy taken by the hadron. In the term depending on x, only contributions from the valence quarks are present.

It is worth mentioning that the QPM formula (1) does not account for a hidden x dependence of $D_f^h(z)$. In fact fragmentation functions as well as multiplicities were observed to depend on W^2 [16,17], which in turn is related to x. The increase of multiplicities with W^2 is about the same for hadrons of opposite charges [18], such that in the formulae (2) the x dependence of the fragmentation functions approximately cancels.

The fragmentation functions used in this analysis are "effective" fragmentation functions, i.e. they contain hadrons produced directly in the fragmentation process as well as those from resonance decays.

Equations (2) are valid at each point in (x,z). However, due to the limited statistics we have integrated them over z (with the restriction that $x_F > 0$). If one defines the zero order moments

$$M^h(x) = \int_0^1 [N^{h^+}(x,z) - N^{h^-}(x,z)]\, dz ,$$

$$\Delta^h(x) = \int_0^1 [D_u^{h^+}(z) - D_u^{h^-}(z)]\, dz ,$$

one obtains for the proton target the following formulae

$$M_H^\pi(x) = \frac{\frac{1}{9}[4xu_v(x) - xd_v(x)]}{F_2^H(x)} \Delta^\pi \tag{3a}$$

$$M_H^p(x) = \frac{\frac{1}{9}[4xu_v(x) + xd_v(x)]}{F_2^H(x)} \Delta^p \tag{3b}$$

$$M_H^K(x) = \frac{\frac{1}{9}4xu_v(x)}{F_2^H(x)} \Delta^K \tag{3c}$$

The measured distributions M^π, M^p, M^K are thus linear combinations of the fractions

$$f_{u_v}(x) = \frac{\frac{4}{9}xu_v(x)}{F_2^H(x)} \quad \text{and} \quad f_{d_v}(x) = \frac{\frac{1}{9}xd_v(x)}{F_2^H(x)}$$

To extract these fractions from the measured M^h's, it is necessary to know the normalisation factors Δ^π, Δ^p, Δ^K, which do not depend on x nor on the target. To obtain them we have used the data from the deuterium target taking advantage of isospin symmetry for the deuteron and its implications for the corresponding formulae.

For the deuterium target one obtains [15] the following formulae for the moments $M^h(x)$

$$M_D^{\pi}(x) = \frac{\frac{3}{18}[xu_v(x) + xd_v(x)]}{F_2^N(x)} \Delta^{\pi} \quad (4a)$$

$$M_D^{p}(x) = \frac{\frac{5}{18}[xu_v(x) + xd_v(x)]}{F_2^N(x)} \Delta^{p} \quad (4b)$$

$$M_D^{K}(x) = \frac{\frac{4}{18}[xu_v(x) + xd_v(x)]}{F_2^N(x)} \Delta^{K} \quad (4c)$$

where the index D refers to deuterium, $F_2^N(x)$ is the isoscalar nucleon structure function (the average of the proton and neutron structure functions) and $u_v(x)$, $d_v(x)$ are the valence quark distribution functions in the proton. The x dependence of the three moments M_D^{π}, M_D^{p}, M_D^{K}, is seen to be the same. Their normalisation is determined by the moments Δ^{π}, Δ^{p}, Δ^{K}. At sufficiently large x values, where the sea quark contribution to the structure function can be neglected, $F_2^N \approx \frac{5}{18}[xu_v(x) + xd_v(x)]$, such that the M_D^h's are constant. To determine the moments Δ^h we have fitted simultaneously to the pion, kaon and proton data for the deuterium the following formula

$$M_D^h(x) = C_h \frac{x^{\alpha}}{1 + \gamma(1-x)^{\beta}} \Delta^h \quad (5)$$

where $h = \pi, p, K$. The C_h are known constants ($C_{\pi} = 3/5$, $C_p = 1$, $C_K = 4/5$) and α, β, γ, Δ^{π}, Δ^{p}, Δ^{K} are the fitted parameters. The fits are performed in the range $0.1 < x < 0.5$.

The moments Δ^h obtained as the limits of $M_D^h(x) / C_h$ for $x \to 1$ are then inserted into the formulae (3) to extract the fractions f_{u_v} and f_{d_v}. Equations (3a), (3b) can be used to extract, in principle, both fractions f_{u_v} and f_{d_v} from the data on pions and protons, whereas equation (3c), for kaons, gives an independent estimate of f_{u_v}. However, it turns out that the determination of $f_{d_v}(x)$, and in consequence of $xd_v(x)$, is not feasible in practice due to the large statistical errors. This results from the fact that f_{d_v} is expressed as a difference of $M^p(x)$ and $M^\pi(x)$, each one of which in turn is also a difference of distributions.

Finally, to obtain $xu_v(x)$ from $f_{u_v}(x)$ one needs to know the structure function $F_2(x)$. For this purpose we have used a parameterisation for F_2 which describes the proton structure function measured in a previous muon-nucleon experiment [19].

It is worth mentioning that whereas both $xu_v(x)$ and $F_2(x)$ evolve with Q^2, the Q^2 dependence of $f_{u_v}(x)$ is much weaker except for the region of the smallest x, where the contribution of the sea quarks to F_2 becomes large. The $xu_v(x)$ distribution is given at $Q^2 = 20\ GeV^2$, which is the mean Q^2 value for the analysed data.

For the purposes of the present analysis only hadrons emitted in the forward hemisphere ($x_F > 0$) were accepted. This cut was made to suppress contributions from target fragmentation, i.e. from the fragmentation of a partonic system left after a single quark was knocked out of the nucleon.

In the definitions of the moments $M^h(x)$ and Δ^h the lower limit of the integrals could be set to any number z_o, $0 < z_o < 1$. It has been checked that for different choices for z_o ($z_o = 0, 0.1, 0.2$) the results are practically the same.

An advantage of using the data from hydrogen and deuterium treated in the same way, is that systematic errors on the normalisation of the hadronic distributions, especially the errors in the particle identification, almost cancel for the extracted fraction $f_{u_v}(x)$.

The described method of extracting the valence quark distribution was tested [15] using a Monte Carlo program. Events were generated according to the Lund model such that for each target about 200,000 events satisfied the kinematical cuts used for the experimental data and then $xu_v(x)$ was extracted from the hadron distributions. The first estimate was obtained using the pion and proton data, the second one from the kaon data. These distributions were compared to the parameterisation of the u valence quark distribution of ref. [20] which was used as input in the Monte Carlo program. Taking into account the statistical errors of the Monte Carlo samples the agreement between the extracted and input distributions was found to be satisfactory.

The measured $M_D^h(x)$ distributions for the deuterium target are shown in fig. 2. The curves are those given by the formulae (5) fitted to the data to obtain the normalisation factors Δ^h's. The fitted values of the Δ^h's are

$$\Delta^{\pi} = \int_0^1 [D_u^{\pi^+}(z) - D_u^{\pi^-}(z)]\, dz = 0.382 \pm 0.031$$

$$\Delta^{p} = \int_0^1 [D_u^{p}(z) - D_u^{\bar{p}}(z)]\, dz = 0.047 \pm 0.011$$

$$\Delta^{K} = \int_0^1 [D_u^{K^+}(z) - D_u^{K^-}(z)]\, dz = 0.122 \pm 0.023$$

As discussed earlier, the above moments are estimated using forward going hadrons ($x_F > 0$) only.

The $xu_v(x)$ distributions obtained from the pion and proton data ($xu_v^{\pi,p}$) and independently from the kaon data (xu_v^{K}), are shown in fig. 3a, 3b and the weighted average of these two distributions is given in fig. 3c. The curve is the $xu_v(x)$ parameterisation of ref. [21] evaluated at $Q^2 = 20$ GeV^2 using the averaged valence quark densities and the CHARM gluon density. The measured $xu_v(x)$ distributions are also listed in table 2.

The errors are the statistical errors of the hydrogen data. The errors of the Δ^h's lead to additional errors, not shown in the figures, which are about 12% for $xu_v^{\pi,p}$ and about 20% for xu_v^{K}. The normalisation error on $F_2(x)$ introduces the systematic normalisation error on $xu_v(x)$ equal to about 5%.

To estimate the systematic error due to the assumption $D_u^p = D_d^p$ an analogous analysis with the assumption $D_u^p = 2D_d^p$ was performed [15] and the results were compared to those presented in fig. 3. The assumption $D_u^p = 2D_d^p$ leads to values of $xu_v(x)$ lower by about 1.5% at small x and by about 3% at large x. This error is thus negligible when compared to the statistical errors.

The systematic errors of the hadron distributions are very similar for the hydrogen and deuterium data and almost cancel for the $xu_v(x)$ distribution.

The distribution $xu_v^{\pi,p}$ obtained in this experiment is compared in fig. 4 to the distributions obtained in inclusive deep-inelastic neutrino-nucleon [3] and muon-nucleon [2] experiments. The two last distributions were measured at $Q^2 = 15$ GeV^2. The $xu_v(x)$ distributions determined in different experiments agree with each other within an accuracy of about 15%. The agreement of our result with the inclusive experiments provides an additional support for the quark-parton model.

4. THE U QUARK FRAGMENTATION FUNCTIONS INTO CHARGED HADRONS

In order to extract the fragmentation functions from the hadron distributions we have used the QPM formula (1). However, this expression does not take into account the observed W^2 dependence [16,17] of the hadron distributions. In the framework of QCD, the evolution of the hadron longitudinal momentum distributions with W^2 is due to interactions in which a hard gluon is emitted by the scattered quark or to interactions proceeding through the photon-gluon fusion mechanism.

To suppress the effects of scale breaking on the fragmentation functions we have selected a kinematic range for the event variables, where these effects are small and consequently where formula (1) can be applied. To define this range we have used a version of the Lund Monte Carlo program in which the leading order QCD processes were described according to the calculations of Altarelli and Martinelli [22].

From these studies we have chosen the cuts $x > 0.12$ and $16 < W^2 < 200$ GeV^2. With these cuts the contribution of the "QCD type events" (i.e. hard gluon emission or photon-gluon fusion) in the sample is always smaller than 10% in any region of x and W^2, and on average their contribution is smaller than 5%. After these cuts the number of events is reduced to 9654 for the hydrogen target and 7476 for the deuterium target.

Fragmentation functions are thus obtained for the following average values of the event variables: $\langle W^2 \rangle = 80$ GeV^2, $\langle Q^2 \rangle = 25$ GeV^2 and $\langle x \rangle = 0.25$.

To extract the fragmentation functions we have considered contributions from the u, d and s quarks and the corresponding antiquarks in formula (1) and we have used the Glück, Hoffmann and Reya parameterisations of quark distributions [20].

The number of independent fragmentation functions has been reduced by applying charge conjugation invariance and isospin rotation symmetry and by the additional relations introduced in section 3, namely $D_d^{K^+} = D_d^{K^-} = D_u^{K^-}$, $D_u^{\bar{p}} = D_d^{\bar{p}}$ and $D_u^p = D_d^p$.

As independent fragmentation functions we have chosen

for pions: $D_u^{\pi^+}$, $D_u^{\pi^-}$, $D_s^{\pi^-}$,

for kaons: $D_u^{K^+}$, $D_u^{K^-}$, $D_s^{K^+}$, $D_s^{K^-}$

for protons: D_u^p, $D_u^{\bar{p}}$, D_s^p, $D_s^{\bar{p}}$.

For the kinematical range chosen in this analysis the contributions from the fragmentation of strange quarks and antiquarks to the hadron distributions are negligible; the fraction of strange quarks $f_s(x) = 1/9\ xs(x)/F_2(x) \approx 0.005$ at $<x> = 0.25$. So the data are insensitive to any particular shape of the strange quark fragmentation functions. In order to simplify the formulae used for the extraction of fragmentation functions, we have made further assumptions concerning the strange quark fragmentation functions:

$$D_s^{\pi^+} = D_u^{\pi^-},\ \frac{1}{2}\left(D_s^{K^+} + D_s^{K^-}\right) = D_u^{K^+},\ \frac{1}{2}\left(D_s^p + D_s^{\bar{p}}\right) = D_u^{\bar{p}}$$

These assumptions have negligible effect on the extracted u quark fragmentation functions $D_u^{h^+}$, $D_u^{h^-}$ $(h = \pi, K, p)$.

Finally, one can relate [15] the normalised hadron distributions $N^h(x,z)$ (see sect. 3 for the definition) to the u quark fragmentation functions $D_u^h(z)$ and fractions $f_f(x)$ of quarks of given flavour f ($f_f(x) = \frac{x\, e_f^2\, q_f(x)}{F_2(x)}$) by the following formulae:

for pions -

$$N^{\pi^+}(x,z) = \left[f_u(x) + f_{\bar{d}}(x)\right] D_u^{\pi^+}(z) + \left[f_{\bar{u}}(x) + f_d(x) + 2f_s(x)\right] D_u^{\pi^-}(z) \ , \tag{6a}$$

$$N^{\pi^-}(x,z) = \left[f_{\bar{u}}(x) + f_d(x)\right] D_u^{\pi^+}(z) + \left[f_u(x) + f_{\bar{d}}(x) + 2f_s(x)\right] D_u^{\pi^-}(z) \ , \tag{6b}$$

for kaons -

$$N^{K^+}(x,z) = \left[f_u(x) + 2f_s(x)\right] D_u^{K^+}(z) + \left[f_{\bar{u}}(x) + f_d(x) + f_{\bar{d}}(x)\right] D_u^{K^-}(z) \ , \tag{7a}$$

$$N^{K^-}(x,z) = \left[f_{\bar{u}}(x) + 2f_s(x)\right] D_u^{K^+}(z) + \left[f_u(x) + f_d(x) + f_{\bar{d}}(x)\right] D_u^{K^-}(z) \ , \tag{7b}$$

and for protons and antiprotons -

$$N^{p}(x,z) = \left[f_u(x) + f_d(x)\right] D_u^{p}(z) + \left[f_{\bar{u}}(x) + f_{\bar{d}}(x) + 2f_s(x)\right] D_u^{\bar{p}}(z) \ , \tag{8a}$$

$$N^{p}(x,z) = \left[f_{\bar{u}}(x) + f_{\bar{d}}(x)\right] D_u^{p}(z) + \left[f_u(x) + f_d(x) + 2f_s(x)\right] D_u^{p}(z) \ . \tag{8b}$$

To extract the fragmentation functions D_u^h, the experimental hadron distributions $N^h(x,z)$ were averaged over the measured x range. It should be mentioned that there exists a weak correlation between the variables z and x, which leads to a slight increase of the average x with increasing z, e.g. $\langle x \rangle = 0.21$ at $z = 0.03$ whereas $\langle x \rangle = 0.27$ at $z = 0.84$. For this reason, for each z point the fractions $f_f(x)$ were taken at the average x value for this particular z.

As in the analysis presented in the preceding section only hadrons emitted in the forward hemisphere ($x_F > 0$) were used in this analysis.

The method of extracting the fragmentation functions was tested using events generated by the Lund Monte Carlo program. The fragmentation functions were extracted from the Monte Carlo events and compared to those used in the Monte Carlo program [15]. For the pions and kaons the agreement between the original and extracted fragmentation functions is very good. For the protons the original D_u^p is in general different from D_d^p; they are about equal for $z < 0.4$, but at larger z the ratio D_u^p / D_d^p increases, becoming about 2 for $0.4 < z < 0.6$ and greater than 2 for $0.6 < z < 0.8$. The extracted D_u^p is very close to the original D_u^p, although the assumption $D_u^p = D_d^p$, made in deriving the formulae (8), is not satisfied for the original fragmentation functions. The reason the extracted D_u^p is not very sensitive to the assumption about D_d^p is due to the dominance of the contribution of u quark scattering in the analysed sample ($f_u = 0.84$ for the hydrogen target and $f_u = 0.73$ for the deuterium target at $\langle x \rangle = 0.25$).

Table 3 contains the extracted fragmentation function separately for the hydrogen and deuterium targets as well as the weighted average fragmentation functions. The fragmentation functions from the hydrogen and deuterium data agree within the statistical errors. The weighted average fragmentation functions are also shown in fig. 5.

The quoted errors are the statistical errors including those introduced by the Monte Carlo corrections described in section 2. The statistical errors are about 5% for the fragmentation functions into pions and about 15% for kaons and protons.

The experimental systematic errors are mostly due to the uncertainties of particle identification and they are about 10% for pions and about 15% for kaons and protons. The possible systematic error due to the parameterisation of the quark distribution functions is less than 2% for pions and protons and less than 4% for kaons. In order to estimate a systematic error due to the assumption $D_u^p = D_d^p$, the analysis was repeated with the assumption $D_u^p = 2D_d^p$ [15]. The resulting values of D_u^p change in such a case by about 4% for the hydrogen and by about 8% for the deuterium data, whereas the $D_u^{\bar{p}}$ is not affected.

In fig. 6 the u quark fragmentation functions into pions measured in this experiment are compared to those obtained in the previous experiment [9]. The agreement of both measurements is good.

At small values of z ($z \approx 0.1$) the unfavoured and corresponding favoured fragmentation functions are about equal, i.e. $D_u^{\pi^-} \approx D_u^{\pi^+}$, $D_u^{K^-} \approx D_u^{K^+}$, $D_u^{\bar{p}} \approx D_u^{p}$. At these z values a large fraction of produced hadrons, especially pions, are the products of resonance decays and as such carry little information on the quantum numbers of the scattered quark.

At large z, for the leading hadrons ($z > 0.5$), the probability for the hadron to contain a valence quark with the quantum numbers of the scattered quark is several times bigger than the probability not to contain such a quark. The favoured fragmentation functions are about 3-4 times larger than the unfavoured ones in this range of z.

The ratios $D_u^{K^+} / D_u^{\pi^+}$ and $D_u^{K^-} / D_u^{\pi^-}$ are shown in fig. 7. They clearly show that the fragmentation functions into pions are softer than the fragmentation functions into kaons. This is due, at least in part, to a larger contribution of resonance decay products for pions than for kaons. The values of the ratios at large z are related in the framework of the Lund model to the ratio γ_s / γ_u characterising the relative probability for the creation of a strange quark-antiquark pair in the colour field. The ratios presented are consistent with $\gamma_s / \gamma_u = 0.3$, the value reported in one of our previous analysis [11].

The ratios $D_u^{p} / D_u^{\pi^+}$ and $D_u^{\bar{p}} / D_u^{\pi^-}$ are shown in fig. 8. These results demonstrate a similar trend to that observed in our previous muon-nucleon experiment [8], where at high Bjorken x ($x > 0.2$) and for $z > 0.4$ the ratio of protons to all positive hadrons (p/h^+) exceeds about twice the ratio of antiprotons to all negative hadrons ($\bar{p}/h^-$). This observation was found to disagree with models where it is assumed that the production of proton-antiproton pairs proceeds exclusively through a mechanism of diquark-antidiquark creation. It agrees however with a model [23] in which the baryon and antibaryon do not have to be neighbours in rapidity, the probability to produce a meson between them being defined by an extra parameter.

5. CONCLUSIONS

Using the distributions of identified charged hadrons produced in the deep inelastic muon scattering on hydrogen and deuterium targets, we have applied a new method to extract the scaled-momentum distribution function of the u valence quark in the proton, $xu_v(x)$. This distribution is obtained at $Q^2 = 20$ GeV^2, the average Q^2 value for the data. The agreement of this result with the distribution functions measured in the inclusive muon-nucleon and neutrino-nucleon scattering experiments provides an additional support for the quark-parton model.

Using a sub-sample of the same data in which QCD effects are suppressed, we have extracted the u quark fragmentation functions into charged pions, kaons, protons and antiprotons. This analysis has been limited to the kinematic range $x > 0.12$ and $16 < W^2 < 400$ GeV^2. The comparison of the resulting fragmentation functions shows that those into pions differ from the ones into kaons and protons. In particular, the comparison of the pion and proton fragmentation gives additional information on the baryon production mechanism.

ACKNOWLEDGEMENTS

We would like to thank all people in the various laboratories who contributed to the construction, operation and analysis of this experiment. The support of the CERN staff in operating the SPS, muon beam and computer facilities is greatly acknowledged.

REFERENCES

[1] T. Sloan, Proc. Int. Europhysics Conf. on High Energy Physics, Uppsala 1987, p.857;
J. Feltesse, Proc. Int. Europhysics Conf. on High Energy Physics, Bari 1985, p. 979.

[2] EMC, J.J. Aubert et al., Nucl. Phys. B293 (1987) 740.

[3] CDHS collaboration, H. Abramowicz et al., Z. Phys. C25 (1984) 29.

[4] WA25 collaboration, D. Allasia et al., Phys. Lett. 135B (1984) 231;
WA25 collaboration, D. Allasia et al., Z. Phys. C28 (1985) 321.

[5] For review see for example: A. Barbaro-Galtieri, Proc. XV Int. Symp. on Multiparticle Dynamics, Lund 1984, p. 678.

[6] J.M. Izen, Proc. XV Int. Symp. on Multiparticle Dynamics, Lund 1984, p.727.

[7] P. Allen et al., Nucl. Phys. B214 (1983) 369.

[8] C. Benchouk, Thèse de troisième cycle, Université d'Aix-Marseille II, 1983;
EMC, J.J. Aubert et al., Phys. Lett. 135B (1984) 225.

[9] EMC, J.J. Aubert et al., Phys. Lett. 160B (1985) 417.

[10] EMC, M. Arneodo et al., Phys. Lett. 150B (1985) 458.

[11] EMC, M. Arneodo et al., Z. Phys. C34 (1987) 283.

[12] EMC, M. Arneodo et al., Z. Phys. C35 (1987) 433.

[13] EMC, O.C. Allkofer et al., Nucl. Instrum. Methods 179 (1981) 445;
EMC, J.P. Albanese et al., Nucl. Instrum. Methods 212 (1983) 111.

[14] B. Andersson, G. Gustafson and C. Peterson, Z. Phys. C1 (1979) 105;
B. Andersson and G. Gustafson, Z. Phys. C3 (1980) 223;
B. Andersson et al., Z. Phys. C9 (1981) 233;
G. Ingelman and T. Sjostrand, preprint LU-TP 80-12 (1980).

[15] C. Benchouk, Thèse de Doctorat d'Etat, Université d'Aix-Marseille II, 1986.

[16] EMC, J.J. Aubert et al., Z. Phys. C31 (1986) 175;
EMC, J.J. Aubert et al., Phys. Lett. 114B (1982) 373.

[17] EMC, M. Arneodo et al., Nucl. Phys. B258 (1985) 249.

[18] EMC, M. Arneodo et al., Z. Phys. C31 (1986) 1.

[19] EMC, J.J. Aubert et al., Nucl. Phys. B259 (1985) 189.

[20] M. Glück, E. Hoffmann and E. Reya, Z. Phys. C13 (1982) 119.

[21] M. Diemoz et al., Z. Phys. C39 (1988) 21;
G. Martinelli, private communication.

[22] G. Altarelli and G. Martinelli, Phys. Lett. 76B (1978) 89.

[23] G. Ingelman, Proc. XV Int. Symp. on Multiparticle Dynamics, Lund 1984, p. 664.

Table 1

Numbers of identified charged hadrons

Particle	H_2 Target			D_2 Target		
	N_{tot}	$N(x_F < 0)$	$N(x_F > 0)$	N_{tot}	$N(x_F < 0)$	$N(x_F > 0)$
π^+	33676	7883	25793	25732	6076	19656
K^+	1891	635	1256	1510	543	967
p	4189	2660	1529	2979	1840	1139
π^-	30368	7492	22876	24640	6270	18370
K^-	1509	562	947	1313	498	815
$\bar{p}$	1395	389	1006	1128	277	861

Table 2

Values of the $xu_v(x)$ distributions extracted from pion and proton data ($xu_v^{\pi,p}$), from kaon data (xu_v^K) and their average. The errors given are the statistical errors.

x	$xu_v^{\pi,p}(x)$	$xu_v^K(x)$	$xu_v^{\pi,p,K}(x)$
0.030	0.304 ± 0.075	0.039 ± 0.111	0.222 ± 0.062
0.072	0.425 ± 0.067	0.490 ± 0.107	0.444 ± 0.060
0.123	0.473 ± 0.069	0.281 ± 0.117	0.423 ± 0.060
0.174	0.658 ± 0.076	0.492 ± 0.118	0.610 ± 0.064
0.242	0.580 ± 0.058	0.548 ± 0.095	0.571 ± 0.050
0.341	0.461 ± 0.061	0.367 ± 0.078	0.425 ± 0.048
0.440	0.279 ± 0.063	0.230 ± 0.070	0.257 ± 0.047

Table 3

The measured u quark fragmentation functions from the hydrogen and deuterium data and the averaged fragmentation functions as functions of the energy fraction z. The errors given are the statistical errors.

	z	H_2 Target	D_2 Target	Average
$D_u^{\pi^+}$	0.03	3.485 ± 0.120	3.519 ± 0.180	3.495 ± 0.100
	0.07	5.746 ± 0.169	5.976 ± 0.247	5.819 ± 0.139
	0.12	4.262 ± 0.145	3.897 ± 0.204	4.139 ± 0.118
	0.17	2.835 ± 0.116	2.922 ± 0.171	2.862 ± 0.096
	0.24	1.736 ± 0.063	1.736 ± 0.090	1.736 ± 0.051
	0.35	0.825 ± 0.042	1.040 ± 0.066	0.886 ± 0.035
	0.45	0.523 ± 0.034	0.582 ± 0.050	0.542 ± 0.028
	0.55	0.275 ± 0.024	0.318 ± 0.037	0.288 ± 0.020
	0.65	0.196 ± 0.021	0.139 ± 0.025	0.172 ± 0.016
	0.75	0.094 ± 0.015	0.075 ± 0.020	0.087 ± 0.012
	0.85	0.051 ± 0.010	0.032 ± 0.013	0.044 ± 0.008
$D_u^{\pi^-}$	0.03	2.871 ± 0.108	2.744 ± 0.162	2.832 ± 0.090
	0.07	5.089 ± 0.159	4.424 ± 0.223	4.866 ± 0.129
	0.12	3.294 ± 0.128	3.444 ± 0.193	3.340 ± 0.107
	0.17	2.031 ± 0.102	2.020 ± 0.152	2.028 ± 0.084
	0.24	1.033 ± 0.051	1.057 ± 0.078	1.040 ± 0.042
	0.35	0.448 ± 0.033	0.396 ± 0.053	0.434 ± 0.028
	0.45	0.224 ± 0.025	0.209 ± 0.038	0.220 ± 0.021
	0.55	0.091 ± 0.016	0.108 ± 0.028	0.095 ± 0.014
	0.65	0.046 ± 0.013	0.061 ± 0.022	0.050 ± 0.011
	0.75	0.033 ± 0.010	0.079 ± 0.021	0.042 ± 0.009
	0.85	0.013 ± 0.007	0.050 ± 0.018	0.019 ± 0.007
$D_u^{K^+}$	0.08	0.456 ± 0.109	0.363 ± 0.243	0.448 ± 0.099
	0.13	0.396 ± 0.086	0.610 ± 0.151	0.448 ± 0.075
	0.18	0.678 ± 0.098	0.543 ± 0.104	0.614 ± 0.071
	0.25	0.425 ± 0.043	0.457 ± 0.063	0.436 ± 0.036
	0.35	0.238 ± 0.029	0.287 ± 0.044	0.253 ± 0.024
	0.45	0.167 ± 0.026	0.167 ± 0.035	0.167 ± 0.021
	0.55	0.093 ± 0.021	0.125 ± 0.033	0.102 ± 0.018
	0.65	0.055 ± 0.017	0.113 ± 0.042	0.064 ± 0.016
	0.75	0.054 ± 0.023	0.019 ± 0.024	0.038 ± 0.017

$D_u^{K^-}$	0.08	0.424 ± 0.095	1.154 ± 0.288	0.496 ± 0.090
	0.13	0.312 ± 0.063	0.460 ± 0.098	0.355 ± 0.053
	0.18	0.276 ± 0.055	0.289 ± 0.063	0.282 ± 0.041
	0.25	0.133 ± 0.022	0.217 ± 0.036	0.156 ± 0.019
	0.35	0.098 ± 0.018	0.114 ± 0.026	0.103 ± 0.015
	0.45	0.040 ± 0.014	0.071 ± 0.024	0.048 ± 0.012
	0.55	0.021 ± 0.010	0.039 ± 0.017	0.025 ± 0.009
	0.65	0.017 ± 0.012	0.036 ± 0.021	0.022 ± 0.010
	0.75	0.014 ± 0.011	0.028 ± 0.026	0.016 ± 0.010
$D_u^p \times 10$	0.09	0.195 ± 0.098	0.051 ± 0.090	0.117 ± 0.066
	0.13	1.551 ± 0.332	1.617 ± 0.345	1.582 ± 0.239
	0.18	2.205 ± 0.384	2.168 ± 0.441	2.189 ± 0.290
	0.25	2.367 ± 0.253	1.604 ± 0.230	1.949 ± 0.170
	0.35	2.270 ± 0.251	2.265 ± 0.288	2.268 ± 0.189
	0.45	1.132 ± 0.151	0.819 ± 0.140	0.964 ± 0.103
	0.55	0.676 ± 0.106	0.551 ± 0.145	0.619 ± 0.078
	0.65	0.435 ± 0.093	0.360 ± 0.095	0.398 ± 0.067
	0.75	0.244 ± 0.064	0.165 ± 0.051	0.195 ± 0.040
	0.85	0.064 ± 0.026	0.094 ± 0.040	0.073 ± 0.022
$D_u^{\bar{p}} \times 10$	0.09	0.118 ± 0.083	0.129 ± 0.111	0.122 ± 0.066
	0.13	1.128 ± 0.265	0.928 ± 0.259	1.026 ± 0.185
	0.18	1.545 ± 0.297	1.991 ± 0.405	1.701 ± 0.239
	0.25	1.202 ± 0.175	1.133 ± 0.200	1.172 ± 0.132
	0.35	0.389 ± 0.102	0.445 ± 0.113	0.414 ± 0.076
	0.45	0.242 ± 0.069	0.269 ± 0.108	0.280 ± 0.058
	0.55	0.128 ± 0.058	0.175 ± 0.070	0.147 ± 0.045
	0.65	0.021 ± 0.025	0.098 ± 0.070	0.030 ± 0.023
	0.75	0.058 ± 0.039	0.105 ± 0.058	0.073 ± 0.032
	0.85	0.010 ± 0.010	0.078 ± 0.057	0.012 ± 0.010

FIGURE CAPTIONS

Fig. 1 Analysis acceptance as a function of x_F for different identified hadrons.

Fig. 2 Experimental distributions of the moments $M_D^{\pi}(x), M_D^{K}(x), M_D^{p}(x)$ for the deuterium target and fitted formulae (5). The errors shown are the statistical errors.

Fig. 3 The $xu_v(x)$ distributions extracted from the experimental data. a) From the pion and proton data ($xu_v^{\pi,p}$). b) From the kaon data (xu_v^{K}). c) Weighted average of $xu_v^{\pi,p}$ and xu_v^{K}. The errors shown are the statistical errors. The curve is the $xu_v(x)$ parameterisation of ref. [21].

Fig. 4 $xu_v^{\pi,p}(x)$ from this experiment compared to the results from inclusive lepton-nucleon scattering experiments [2], [3].

Fig. 5 Fragmentation functions of the u quark into pions (a), kaons (b) and protons (c) vs. the energy fraction z. The errors shown are the statistical errors.

Fig. 6 Fragmentation functions of the u quark into pions measured in this experiment and in the experiment [9]. The errors shown are the statistical errors.

Fig. 7 Ratios of the u quark fragmentation functions into kaons and pions vs. the energy fraction z. The errors shown are the statistical errors.

Fig. 8 Ratios of the u quark fragmentation functions into protons and pions vs. the energy fraction z. The errors shown are the statistical errors.

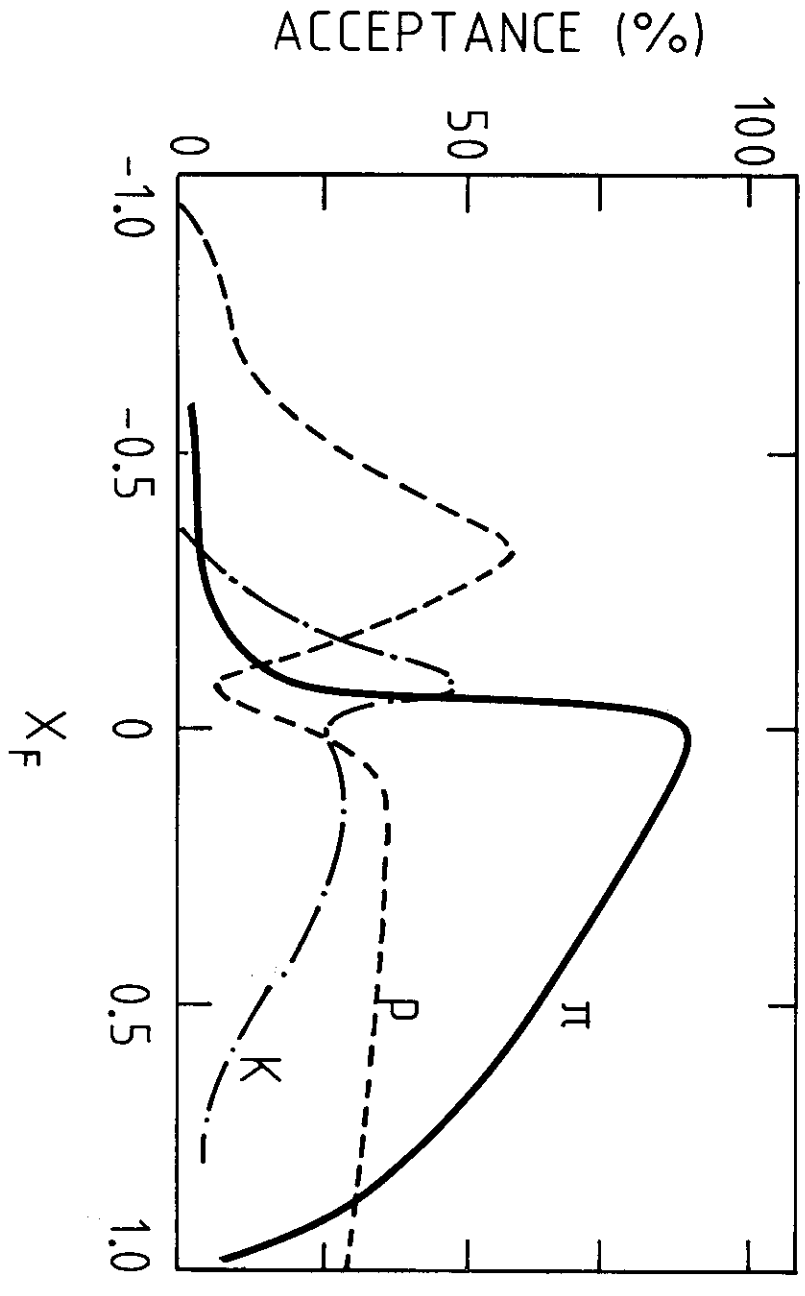

FIG. 1

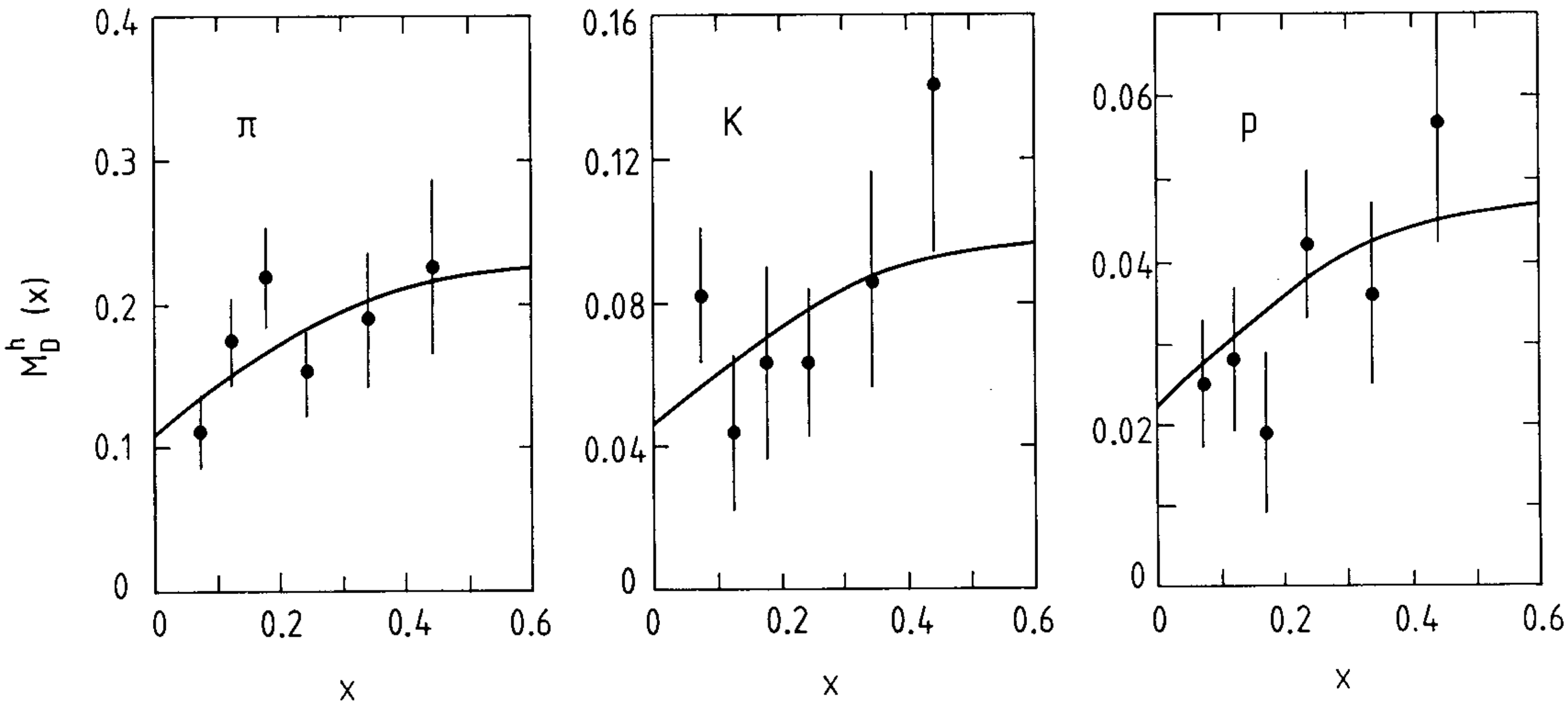

FIG. 2

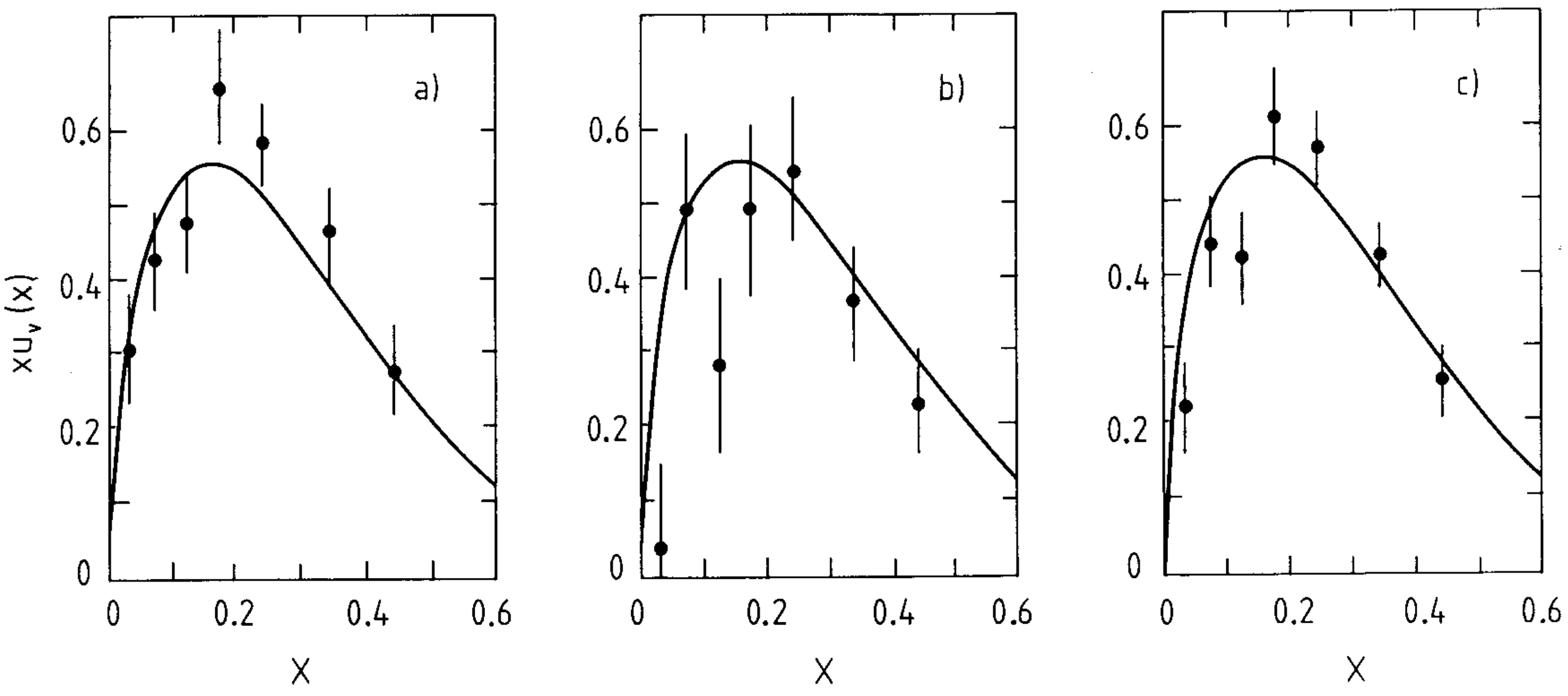

FIG. 3

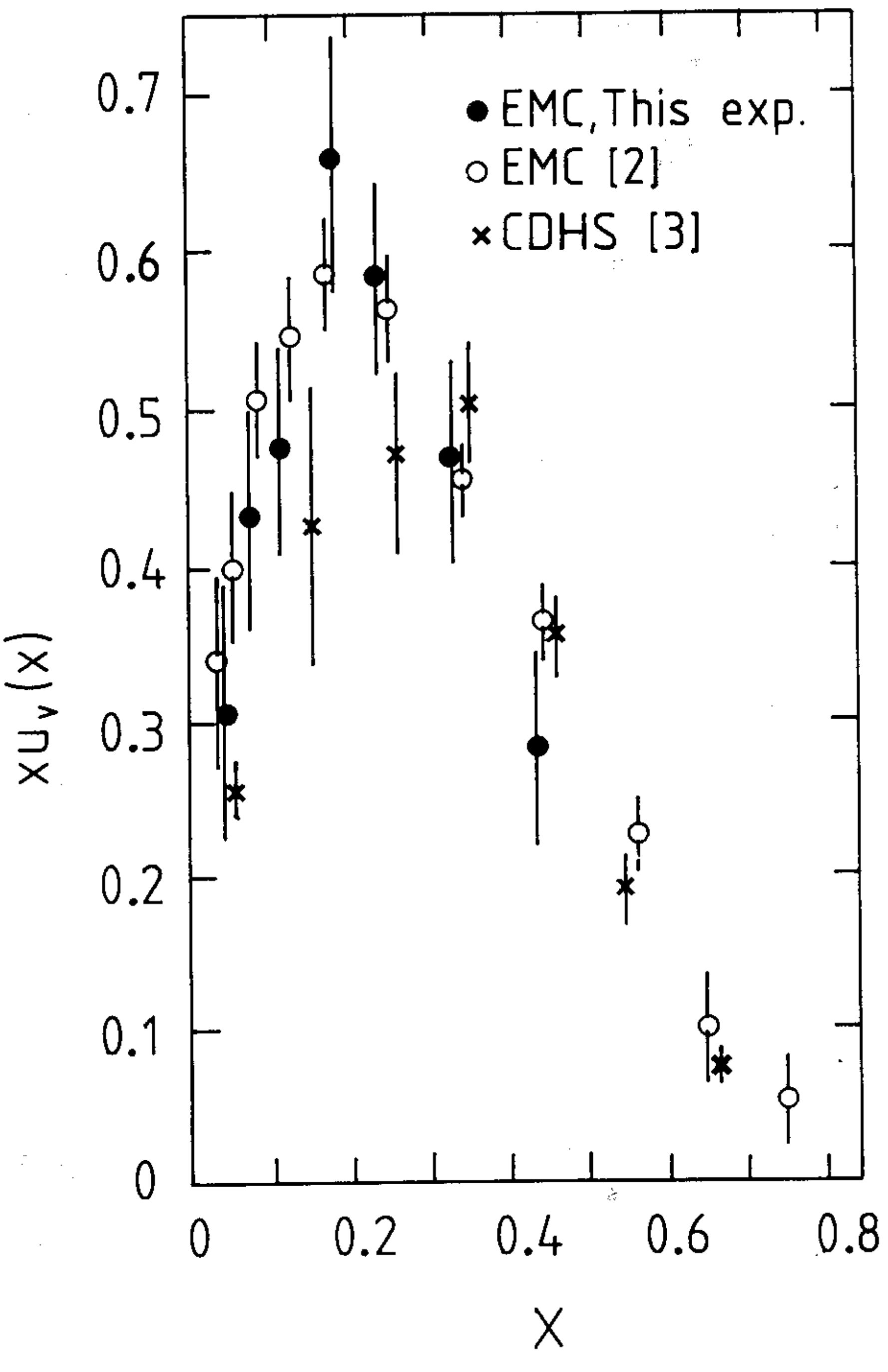

FIG. 4

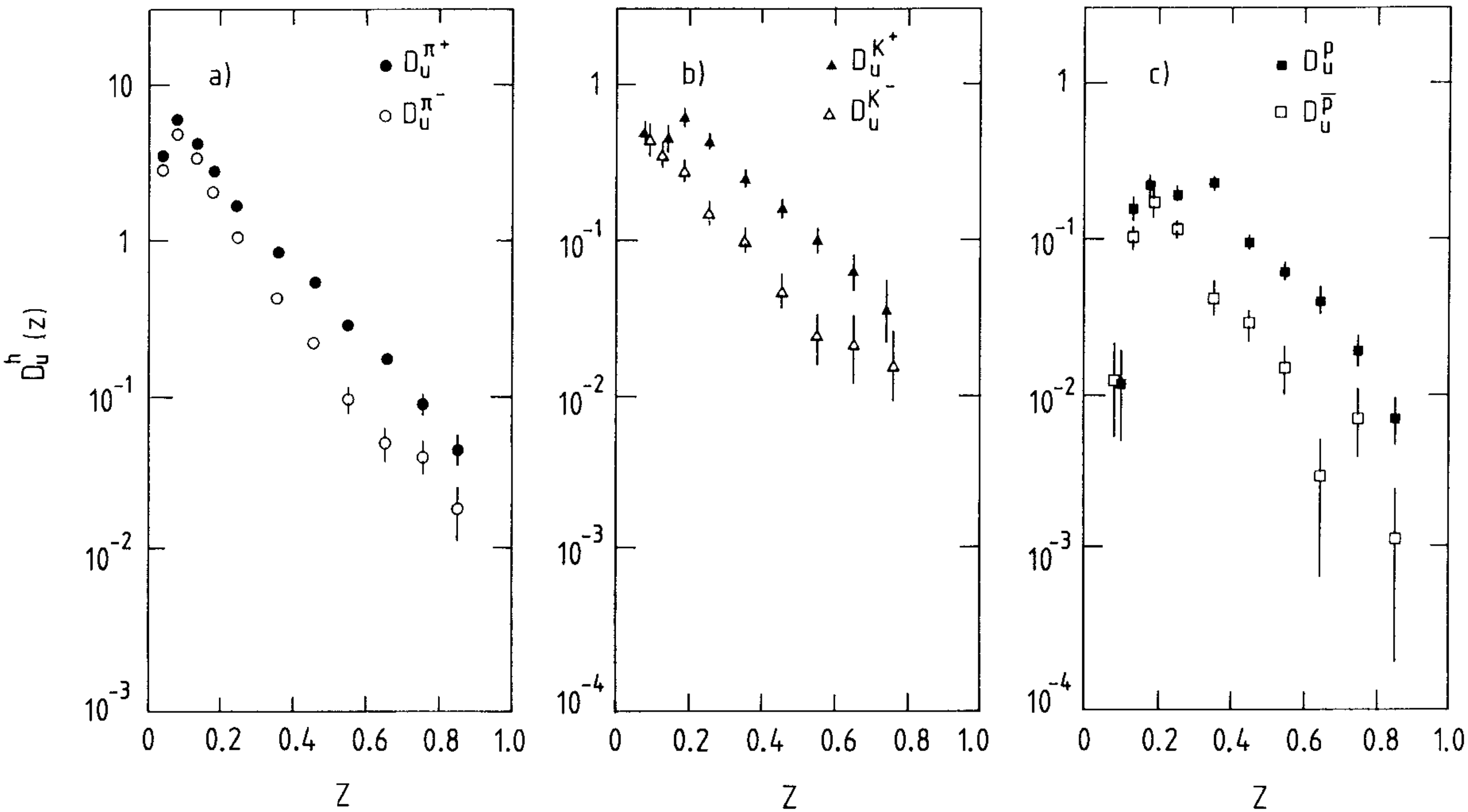

FIG. 5

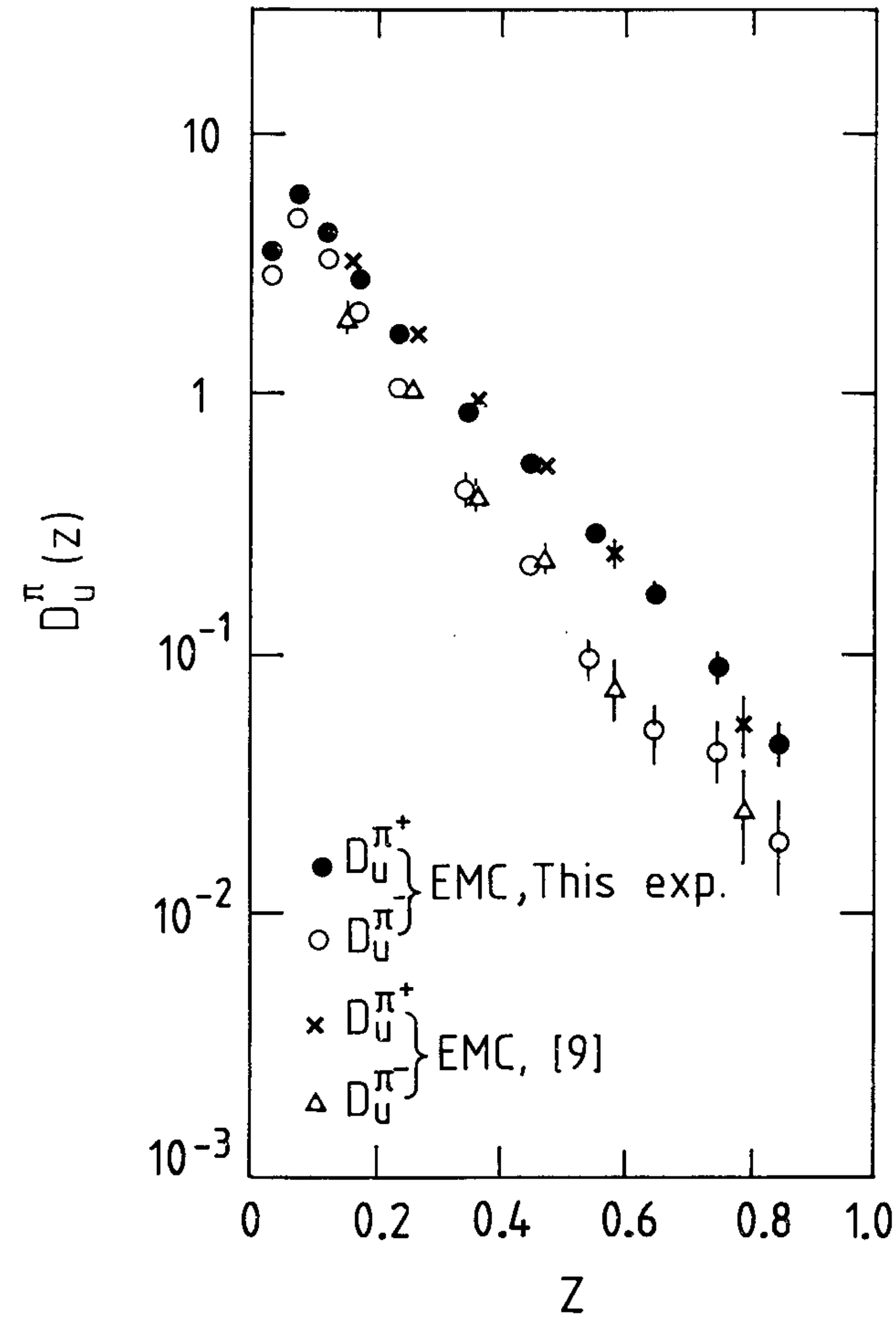

10
1
10^{-1}
10^{-2}
10^{-3}
$D_u^{\pi}(z)$
$D_u^{\pi^+}$
$D_u^{\pi^-}$
EMC, This exp.
$D_u^{\pi^+}$
$D_u^{\pi^-}$
EMC, [9]
0
0.2
0.4
0.6
0.8
1.0
Z

FIG. 6

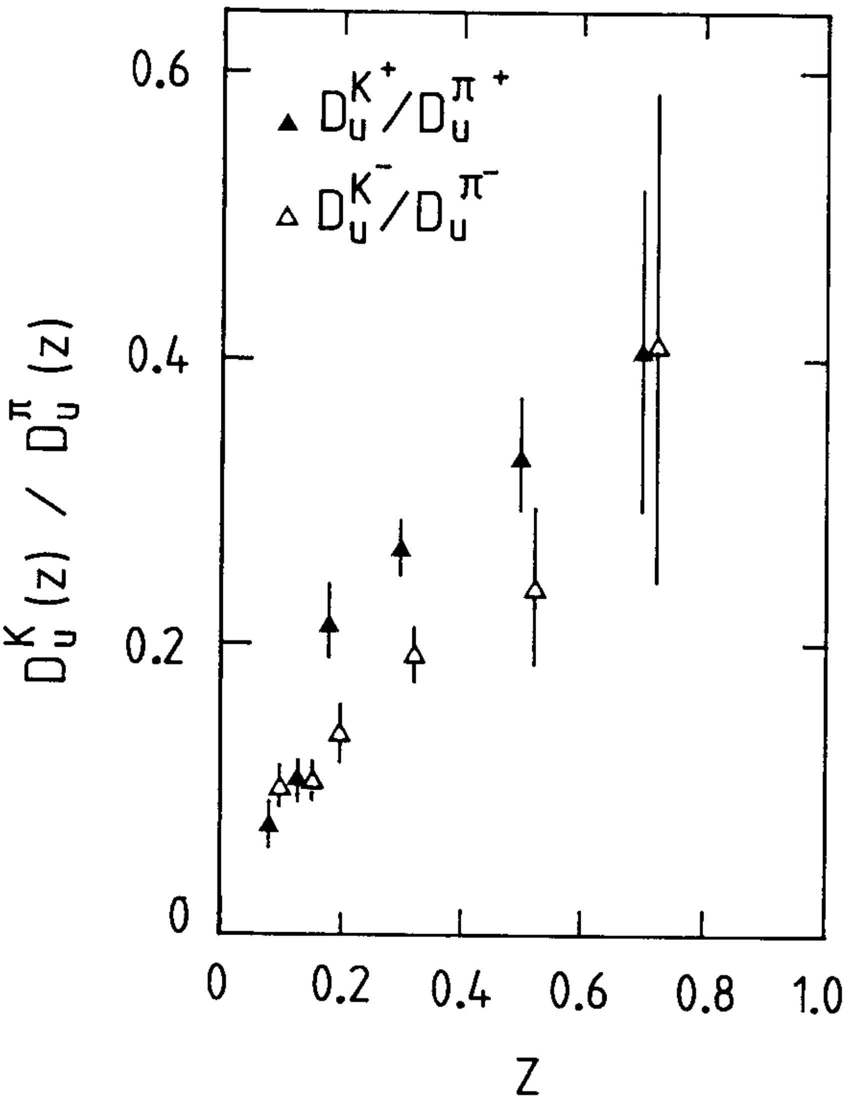

FIG. 7

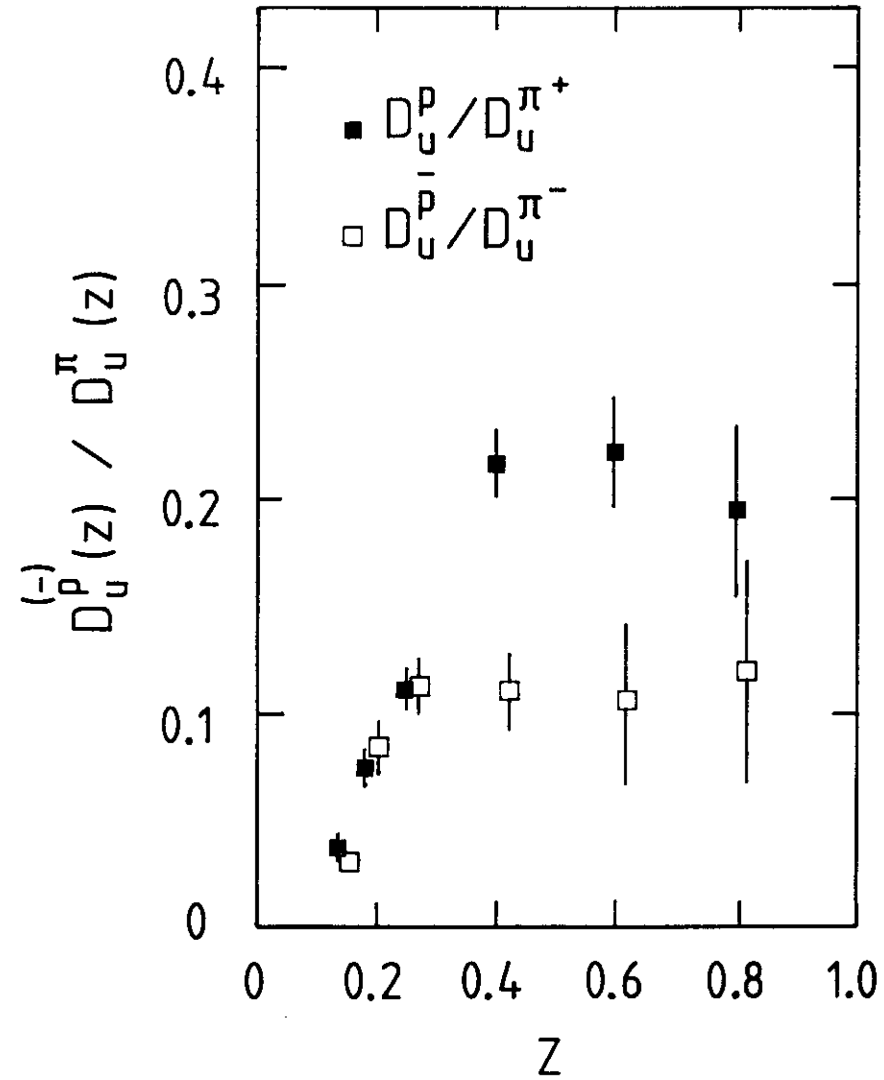

0.4
0.3
0.2
0.1
0
$D_u^p / D_u^{\pi^+}$
$D_u^{\bar{p}} / D_u^{\pi^-}$
$D_u^{\overset{(-)}{p}}(z) \;/\; D_u^{\pi}(z)$
0
0.2
0.4
0.6
0.8
1.0
Z

FIG. 8